Eur Biophys J (2004) 33: 121–129
DOI 10.1007/s00249-003-0359-y

ARTICLE

A. Budi · S. Legge · H. Treutlein · I. Yarovsky

Effect of external stresses on protein conformation: a computer modelling study

Received: 13 March 2003 / Revised: 27 August 2003 / Accepted: 28 August 2003 / Published online: 23 October 2003

Abstract The increasing use of digital technologies such as mobile phones has led to major health concerns about the effects of non-ionizing pulsed radiation exposure. We believe that the health implications of exposure to radiation cannot be fully understood without establishing the molecular mechanisms of biological effects of pulsed microwaves. We aim to establish methods for studying the molecular mechanisms of protein structural and energetic changes occurring due to external stresses related to non-ionizing radiation by using a combination of experimental and theoretical approaches. In this paper, we present the results from our fully atomistic simulation study of chemical and thermal stress response of a prototype protein, insulin. We performed a series of molecular dynamics simulations of insulin in solution under equilibrium conditions, under chemical stress (imitated by reducing the disulfide bonds in the protein molecule), and under short-lived thermal stress (imitated by increasing simulation temperature for up to 2 ns). The resultant protein conformational behaviour was analysed for various properties with the aim of establishing analysis routines for classification of protein unfolding pathways and associated molecular mechanisms.

Keywords Conformational analysis · Insulin · Molecular dynamics simulations · Non-ionizing radiation · Protein unfolding

Submitted as a record of the 2002 Australian Biophysical Society meeting

A. Budi · S. Legge · I. Yarovsky (✉)
Department of Applied Physics, RMIT University, GPO Box 2476V, 3001 Melbourne, Victoria, Australia
E-mail: irene.yarovsky@rmit.edu.au
Tel.: +61-3-99252571
Fax: +61-3-99255290

H. Treutlein
Cytopia Pty. Ltd., Level 5, Baker Institute, Commercial Road, 3004 Melbourne, Victoria, Australia

Introduction

The function of a protein is intrinsically associated with its three-dimensional conformation. Therefore, any changes in the geometry of the protein, particularly in the region of the active site, have the potential to alter its biological function. Previous experiments have shown that there are links between external stress, such as electromagnetic fields, and protein structure. In several reported cases, the presence of weak microwave fields was enough to induce physiological changes in organisms (de Pomerai et al. 2002; French et al. 2000). Although the use of electromagnetic fields as a stressor has been investigated (Bohr and Bohr 2000; de Pomerai et al. 2002; French et al. 1997), these experimental studies were done via directly observable tissue damage, i.e. at long experimental timescales and relatively large length (size) scales. Therefore, the exact cause of these physiological changes, and the extent of the contribution of thermal and/or chemical stress to these changes, are not fully understood.

It is now believed that the effect of pulsed microwave radiation may only become apparent at short timescales (within the nanosecond region) and at the microscopic length scale, i.e. at the molecular level (Laurence et al. 2000). Therefore, it may not be possible to apply traditional experimental measurements to identify such short-lived microscopic effects which may cause identifiable physiological changes.

Conformational changes in proteins trigger the expression of small heat shock response proteins (sHSPs) as part of a defence mechanism used by the cell. The sHSPs are molecular chaperones that either assist in the refolding of the protein or, alternatively, in the degradation of the protein. The expression of sHSPs is not simply a response to heat, but is a general response to other stressors such as alcohol, heavy metals, oxidation, and osmotic pressure changes. The over-expression of sHSPs has been associated with increased oncogenesis and metastasis, as well as increased resistance to

anticancer drugs (French et al. 2000 and references therein). Studies have shown an increase in expression of sHSPs resulting from microwave irradiation, without a measurable temperature rise (Daniells et al. 1998; de Pomerai et al. 2002). Recent work suggests the expression of sHSPs only occurs in a limited range of power absorbed when tissues are exposed to microwaves (Laurence et al. 2000). At low power levels, sHSPs are not activated, resulting in partial unfolding and disruption to protein function. At higher power levels, the sHSPs are expressed and protect the protein from conformational changes that may disrupt their function. At very high power levels, the sHSPs cannot prevent the protein unfolding. This leads to aggregation and precipitation, and therefore cell death.

It is long believed that microwave radiation can only cause thermal heating of the surrounding water, as there is insufficient energy to break even the weak chemical bonds in the proteins. In other words, electromagnetic fields are insufficient to cause chemical stress on proteins (Stuerga and Galliard 1996). However, recent works show evidence of non-thermal effects on proteins (Bohr and Bohr 2000; de Pomerai et al. 2002).

While it may not be possible to utilize traditional experimental measurements to probe the non-thermal as well as short-lived thermal effects, it is possible to employ computer modelling techniques to study protein behaviour at the atomistic level within the nanosecond timeframe under a variety of simulated stress regimes. The relatively long timescale (in simulation terms) of protein unfolding events (microseconds) means that significant progress in the simulation of protein unfolding has only been made within the last few years (Kazmirski and Daggett 1998; Kazmirski et al. 1999; Li and Daggett 1996, 1998; Mayor et al. 2000; Pande and Rohksar 1999; Pastrana-Rios 2001; Snow et al. 2002).

The purpose of our work is to establish computer simulation methods to study protein behaviour in solution under external stresses, such as thermal spikes, chemical changes, and electric field. We also aim at developing analysis routines which will allow us to classify major stages of the protein unfolding pathways, their stability and reversibility as a function of the external conditions. Having access to atomic level information on the protein structure produced by molecular simulation, we will be able to analyse the inter-atomic interactions that are responsible for the observed conformational changes and, hence, establish the molecular mechanisms of protein unfolding under the stress conditions.

Prototype protein: insulin

For this preliminary study we have selected insulin (PDB code 1ZNI) (Bentley et al. 1976) as a prototype for establishing our simulation and analysis procedures. Because of its importance in the treatment of diabetes, the insulin molecule has been the subject of intense study with respect to the characterization of not only its biochemical properties but also its various structural forms. The physiologically active form of the hormone is a monomer; however, the molecule has the ability to combine into associated states, such as dimers, tetramers, and hexamers. Monomeric insulin is a relatively small protein (51 residues) consisting of two chains, A and B, linked by two disulfide bonds (Fig. 1). Chain A is composed of 21 residues with two helices, one at the N-terminus and another at the C-terminus. A single disulfide bond is present, linking residues 6 and 11. The 30-residue chain B contains an N-terminal helix.

Changes are observed in the side-chain and main-chain conformations associated with the oligomerization of insulin, and the conformation is seen to vary between different crystallographic forms (Chothia et al. 1983). Much of the conformational variation is centred within chain B. The secondary structural characteristics of chain B include the N-terminus (B1 to B8), a central α-helix (B9 to B19), a characteristic chain B fold (β-turn from B20 to B23), and the C-terminus (B24 to B28). X-ray crystallographic studies of hexameric and dimeric insulin have shown several conformational states for the N-terminus of chain B (Badger et al. 1991; Bentley et al. 1976; Ciszak et al. 1995; Derewenda et al. 1989; Yao et al. 1999). Motion is also observed in the C-terminus of chain B. Studies of the physiologically active monomeric forms of insulin observed fluctuations in the N-terminus (Hua and Weiss 1991; Olsen et al. 1996; Pittman and Tager 1995) and regions of disorder in the C-terminus (Hua et al. 1991; Ludvigsen et al. 1998; Zhang et al. 2002). Conformational variations were also reported in previous molecular dynamics studies of the monomer and dimer forms of insulin (Falconi et al. 2001; Kruger et al. 1987; Mark et al. 1991). Because of the significant differences in terms of structural resolution, it has been generally postulated that the native insulin monomer is intrinsically flexible, and that this property is integral to the interaction of insulin and its receptor (Hua et al. 1991, 1993a).

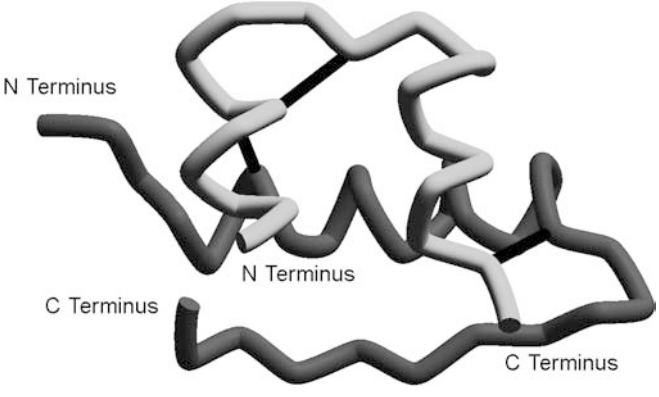

Fig. 1 Schematic representation of insulin. Chain A is coloured *light grey* and chain B is coloured *dark grey*. The disulfide bonds are shown as *black straight lines*

The inherent mobility of chain B of insulin indicates a central role in the activity of the hormone, although the extent of the chain's flexibility is still being determined. Circular dichroism studies of the oxidized chain B report considerable structural disorder in aqueous solution (Du et al. 1982; Wu and Yang 1981). The individual chain B is thought to have the capacity to fold principally without chain A and the associated intrachain disulfide bonds (Hawkins et al. 1995; Qiao et al. 2003). It has also been suggested that chain B acts as a template for the folding of chain A (Hua et al. 2001, 2002; Qiao et al. 2003). Further evidence of the ability of chain B to act independently of chain A has been shown in the determination of the NMR structure of an oxidized chain B (Hawkins et al. 1995). In comparison with the crystal structure, the major structural aspects of the chain were maintained. The central helix was relatively well conserved and so was the β-turn, although slightly shifted in position (B17 to B21). The N- and C-termini were defined as extended β-strands; however, a wide range of conformations for these regions occurred, with the C-terminus region being significantly disordered.

The interaction between the insulin molecule and its receptor is not a well-understood mechanism. There is some evidence to suggest that the observed conformation of native insulin is an artefact of the crystallographic process, where crystal contacts within the packing of the molecules modify the active form of the structure (Dong et al. 2003). Rearrangement of native insulin on binding to its receptor was implied from the observation that the conformation of insulin in the crystal structure is analogous to an inactive form of the molecule (Derewenda et al. 1991). Studies of fully active mutants have revealed perturbation of the C-terminus of chain B (Hua et al. 1993a; Ludvigsen et al. 1998; Mirmira et al. 1991). This raises the issue of the significance of this region's inherent flexibility and its role in the interaction of the insulin molecule with its receptor, and reinforces the need for further investigation of the conformational dynamics of chain B.

In order to establish our analysis routines of protein unfolding, we will focus on the behaviour of chain B of the insulin molecule, exploiting the known flexibility and the structural characteristics of the chain, using MD simulations of the whole molecule in equilibrium and of the isolated chain under chemical and temperature stresses.

Methods

This work has utilized classical molecular dynamics (MD) techniques (Allen and Tildesley 1989; Leach 2001) to explore the mechanism of protein unfolding under various stresses with full atomistic details. The types of stresses have been chosen to represent the previously suggested effects of electromagnetic radiation. In particular, the short-lived temperature stress is modelled because there is evidence that the microwave radiation causes localized, very fast heating within the nanosecond timescale undetectable by traditional thermometry (Laurence et al. 2000). Pulsed temperature rises have also been recently observed in direct microwave exposure experiments on proteins (Berry et al., in preparation). Chemical stress has been modelled here to simulate the suggested athermal effect of radiation (Bohr and Bohr 2000; Laurence et al. 2000).

The chemical stress was imitated by the reduction of all three disulfide bonds in the molecule, effectively isolating the chains from each other. Thermal stress was modelled by the temperature increase to 400 K during the simulation. The thermal stress has been applied to both intact and chemically reduced molecules. The isolated chain B has also been simulated in order to develop analysis procedures for comparison of its unfolding behaviour within different environments. In addition, a reference simulation of the intact insulin at room temperature has been performed to validate the simulations and for comparison with the stressed behaviour. In summary, the following systems have been studied:

1. Complete insulin with all disulfides at 300 K.
2. Complete insulin with all disulfides at 400 K.
3. Complete insulin with no disulfide at 300 K.
4. Complete insulin with no disulfide at 400 K.
5. Isolated chain B at 300 K.
6. Isolated chain B at 400 K.

The NAMD molecular dynamics code was used in this work (Kalé et al. 1999), with well-validated empirical potentials implemented in the CHARMM27 forcefield (MacKerell et al. 1998). CHARMM27 is an all-atom forcefield, which means all atoms in the system are treated explicitly and their interaction potential depends on the individual local atomic environment. We have applied periodic boundary conditions (PBC) to each simulated system using water as solvent with a density of 1.0 g/cm^3. The size of the periodic box was chosen such that the soaked protein had at least a 15 Å thick water layer around it. Since the simulation box was repeated periodically in three dimensions during the simulation, the bulk protein solution is effectively simulated (Allen and Tildesley 1989). An interatomic interaction cut-off distance of 15 Å was chosen to ensure that the protein would not experience self-interaction, which would otherwise complicate, and possibly invalidate, the results. Classical MD simulations were then performed at 300 K and 400 K in the NVT (constant number of particles, constant volume, and constant temperature) ensemble. The length of the simulations for this study was 2 ns using a time step of 1 fs to simulate the proposed short-lived temperature stress. The system details and the simulation parameters are summarized in Table 1.

Results and discussion

The simulated MD trajectories have been analysed for the following properties as a function of the imposed stress conditions: conformational behaviour of the protein, focusing on particular elements of the secondary structure; classification of states in the unfolding pathway; degree of unfolding and structural difference with the native structure; solvent accessible surface area

Table 1 Summary of the systems simulated, and their simulation parameters

System number	Number of water molecules	Temperature (K)	Simulation details
1	6879	300	Velocity Verlet integration;
2		400	PBC box (60 Å×60 Å×60 Å);
3		300	NVT ensemble; potential
4		400	switching at 12 Å; potential
5	7002	300	cut-off at 15 Å
6		400	

changes; hydrogen bond structure; and water mobility. The analyses have been carried out using routines implemented in the VMD (Humphrey et al. 1996), InsightII (InsightII User Guide 1996), X-PLOR (Brünger 1992), and PEPCAT (O'Donohue et al. 2000) software packages. Application and details of the analyses are illustrated below using the insulin chain B trajectories from the systems simulated.

Conformational analysis using PEPCAT

The computer program PEPCAT was used to analyse the effects of chemical and thermal variations on the conformational properties of insulin. PEPCAT is particularly useful in monitoring changes in the specific elements of the secondary structure of proteins (O'Donohue et al. 1995). The conformations from the MD trajectory are processed according to a set of specified geometric descriptors (e.g. atom–atom distances, ϕ and ψ dihedral angles), and subsequently classified into a set of conformational states, based on similarity in the descriptors. The conformational changes that occur during the MD simulation are reflected in the classified states, and can be visualized in conformation transition maps. This enables the unfolding pathways of the protein under different conditions to be characterized and compared.

In this study a particular structural feature of the protein chosen for analysis was the α-helix present in chain B of insulin, whose extent of disordering when placed under stress was determined with PEPCAT. The geometric descriptors used to classify the conformations were five atom–atom (C_α–C_α) distances between the helix residues, detailed in Table 2. The states were identified by a set of all five descriptors' values, where each descriptor can adopt a value of 0, 1, or 2, depending on the imposed distance criteria, specified in Table 2. For example, a descriptor set (0, 0, 0, 0, 0) identifies the native state.

The conformations contained in the trajectory from the 2 ns MD simulations of the systems 5 and 6 were classified according to the geometric descriptors. Both systems are under chemical stress induced by the removal of the interchain disulfide bond and the subsequent isolation of chain B, while system 6 is also subjected to the additional thermal stress at 400 K. It should be emphasized that these systems and conditions were chosen for the purpose of establishing the simulation and analysis routines and should not be considered as representing a realistic insulin environment and behaviour.

Table 2 Details of PEPCAT descriptors used in this work

Descriptor number	Descriptor definition residues	Descriptor values and distance range criteria (Å)		
		0	1	2
1	Gln4–Gly8	< 7	7–9	> 9
2	Gly8–Leu11	< 6	6–8	> 8
3	Leu11–Leu15	< 7	7–9	> 9
4	Leu15–Cys19	< 7	7–9	> 9
5	Gln4–Cys19	< 19	19–22	> 22

The effects of thermal and chemical stress on the conformation of the insulin chain B are illustrated in conformational transition maps presented in Figs. 2 and 3. The circles represent the conformational state, and its area is directly proportional to the population, i.e. the number of simulation frames belonging to that state. The arrows represent the transitions that occur between states, and the width of the arrows is directly proportional to the frequency of transitions to that state.

Figure 2 is a conformational transition map showing the set of conformations (17 states) produced from the simulation of chain B at 300 K. The major conformational state is classified as state 3, and the most frequent transition between conformations occurs between states 3 and 4. The starting structure (state 0) for the simulation is shown in Fig. 4, and can be compared to representative structures from the identified conformational states presented in Fig. 5. The conformations exchanging with state 3 appear to represent equilibrium geometries of the molecule, with numerous transitions to and from the most frequent state 3 conformations. For example, conformational states 2, 4, 7, and 13 all have frequent transitions to state 3. Although the helical structures of states 3 and 4 are predominantly well ordered, the N-terminus region is showing evidence of disruption, which can be seen from the difference in the first geometric descriptor between these states and the starting structure.

When the temperature is elevated to 400 K, an increased number of conformations of chain B is observed (28 states). Figure 3 illustrates the transition map of the classified conformations. The preferred conformation is

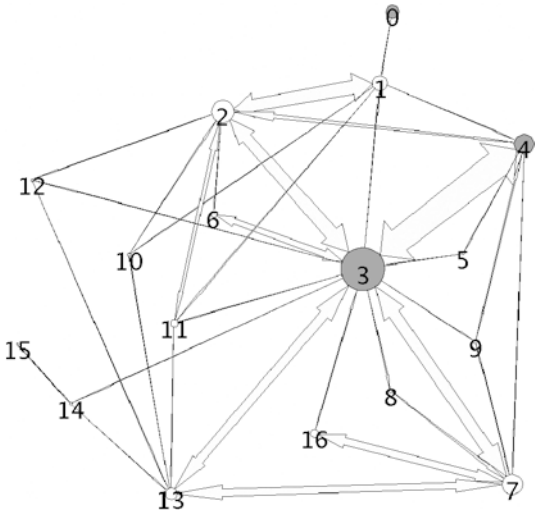

Fig. 2 Conformation transition map for system 5. See accompanying text for further information

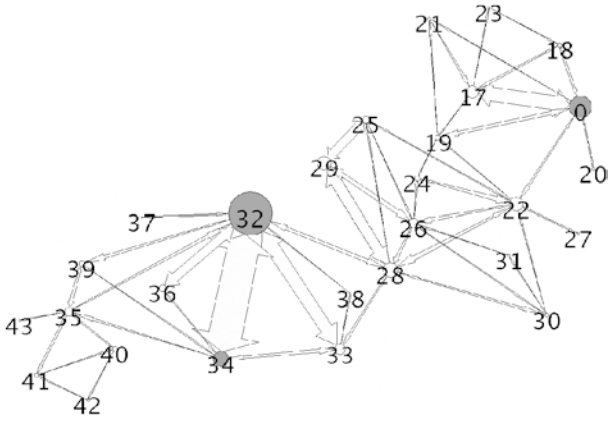

Fig. 3 Conformation transition map for system 6. The emergence of a more distinct transition pathway from the native to a largely disordered state is observed with the increase in temperature of the simulation. See accompanying text for further information

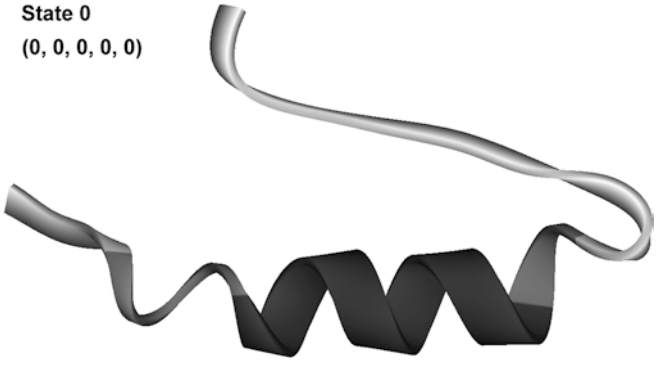

Fig. 4 Conformation state 0. This is the energy minimized structure obtained from the PDB, which is used as the starting geometry for the dynamics simulations

state 32, with frequent fluctuation occurring between states 32 and 34. The transition map at the increased temperature shows possible transition pathways of the denaturation of the protein. A transition pathway is observed between the starting native structure (state 0) and the largely unfolded conformation (state 34), through a highly populated transition state conformation (state 32). The structures of states 32 and 34 are shown in Fig. 5. The structure of state 32 is disordered at the C-terminus region of the helix. In state 34, this disruption is accompanied by loosely structured regions at the N-terminus of the helix. This pattern is reflected in the values of the geometric descriptors used to classify the conformations.

The results suggest that such a classification of the conformational behaviour of proteins under stress is capable of characterizing unfolding pathways under different stress conditions. For example, it can be suggested from the preliminary analysis performed here that chemical stress alone results in smaller conformational changes, with the conformations predominantly centred around one state (state 3), which exhibits only partial unfolding. More dynamic behaviour is observed when thermal stress is added to the system. At 400 K a more significant denaturation of the protein occurs via the classified sequence of transition states.

Root mean square displacement analysis

The purpose of the RMSD analysis was to assess the extent of deviation of the protein structure from the native structure during the MD simulations. RMSD values were calculated for each system by comparing the conformations of the backbone atoms with the experimental structure of 4-zinc insulin (PDB code 1ZNI), aligned on all of the backbone atoms, and discarding the inherently flexible first and last residues to minimize error. The RMSDs presented in Table 3 were averaged over the last 0.5 ns of the simulations.

The RMSD value of around 3.5 Å for the intact insulin molecule at room temperature (system 1) is relatively high (Table 3). This can be further illustrated by a more detailed analysis of the regions of variability of the molecule. In particular, chain B of insulin shows characteristic patterns of deviation from the crystal structure. This can clearly be seen from the overlay and RMSD plot (Fig. 6), which shows the stable α-helix and β-turn, and the change in conformation of the N- and C-termini during the last half nanosecond of the simulation (1.5–2.0 ns). The structures sampled during the MD were aligned along the backbone atoms of the conserved α-helical region (residues 7 to 19). Figure 6 also shows that both termini are quite mobile, especially the C-terminus. These results are in agreement with the experimentally observed conformational changes of the N- and C-termini of the insulin chain B, indicating that the equilibrium simulation (system 1), used to validate the simulation parameters, has reproduced the known flexibility of the protein (Dodson et al. 1983; Hua et al. 1993b; Zhang et al. 2002).

The systems at 400 K (2, 4, 6) changed more significantly than the respective systems at 300 K (1, 3, 5), as expected with an increase in temperature. Not surprisingly, systems 1 and 2, representing the complete insulin molecule with all disulfide bonds intact, are more stable compared to their respective systems without disulfide bonds (systems 3 and 4). System 3 behaves in a similar manner to system 1, where the only difference is the absence of a disulfide bond between chains. This is consistent with the experimental finding that insulin chain B folds without interchain disulfide bonds (Hawkins et al. 1995; Hua et al. 2001). This also indicates that chemical stress alone does not cause very significant changes within the studied timeframe, again consistent with the experimental evidence of the independence of chain B (Hawkins et al. 1995). In contrast, when thermal stress is added to a chemically reduced molecule, as in systems 4 and 6, deviation from the native form occurs. Interestingly, system 6 was particularly unstable, undergoing major conformational changes, which can

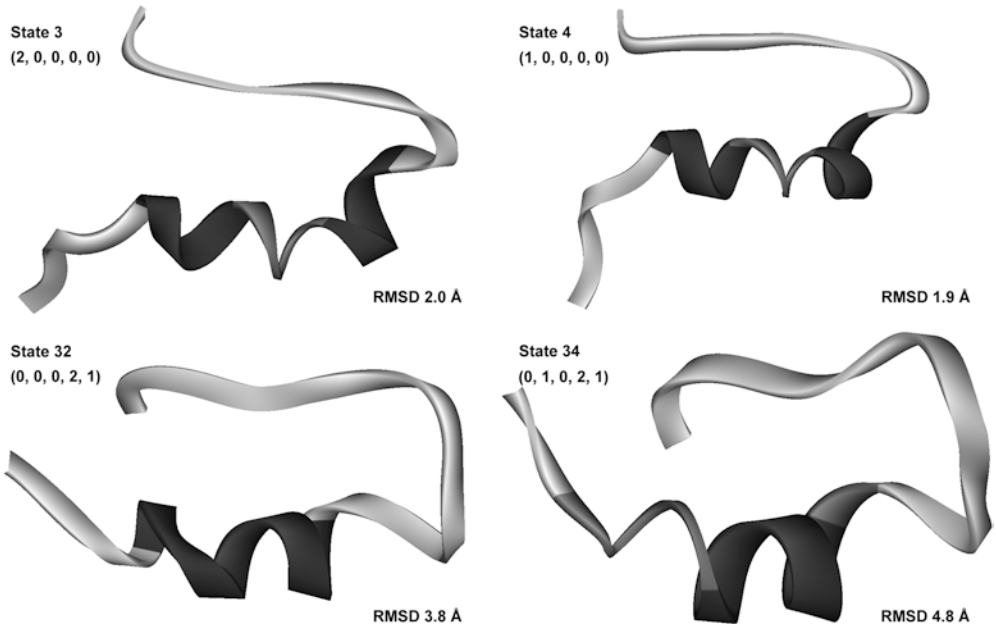

Fig. 5 Representatives of the major conformation states as identified by PEPCAT. The RMSDs (Å) of the backbone atoms between the minimized native structure and the representative PEPCAT identified conformations of insulin chain B are shown. Each conformational state is identified by a distinct set of geometric descriptor values

be attributed to the simultaneous chemical (isolation from chain A) and thermal stresses imposed.

Water mobility

Diffusion constants were calculated from mean square displacements of water molecules during the MD simulations using the Einstein relation (Allen and Tildesley 1989; Leach 2001). Water diffusion constants were obtained for different systems to investigate the mobility of water around the protein in the presence of thermal and/or chemical stresses, as shown in Table 3. We have compared the diffusion constants in the protein systems to the diffusion constants from the bulk water simulations at 300 K and 400 K.

It can be seen that there is almost no difference in the water diffusion rate in systems 1, 3, and 5 as well as in systems 2, 4, and 6. These two groupings are determined by the simulation temperatures of 300 K and 400 K, respectively. Therefore, the diffusion rate increase is due to the thermal motion. This increase has a significant effect on the protein dynamics, which is reflected in the RMSD differences that can be similarly grouped (Table 3). A pure water system was simulated to check the forcefield potentials for water, and an excellent agreement with the experimental water diffusion constant (Hertz 1973) was achieved. Compared to the bulk water systems, the diffusion constants of the protein–water systems are higher by 40% and 30% at 300 K and 400 K, respectively. This increased mobility of water in the presence of the protein can be attributed to the disruption of some hydrogen bonds present in bulk water, causing the water molecules to move more freely.

Table 3 Dynamical properties of the systems following 2 ns of MD simulations, averaged over 1.5–2.0 ns. All of the backbone atoms are used for alignment

System number	RMSD (Å)	Diffusion constant (10^{-5} cm^2/s)
1	3.59 ± 0.25	3.318 ± 0.001
2	5.0 ± 0.5	9.106 ± 0.002
3	3.27 ± 0.15	3.319 ± 0.001
4	6.08 ± 0.55	9.261 ± 0.003
5	3.8 ± 0.2	3.425 ± 0.001
6	11 ± 2	9.315 ± 0.002
Water (at 300 K)		2.336 ± 0.002
Water (at 400 K)		6.961 ± 0.008

Solvent accessible surface area

Analysis of the solvent accessible surface area (SASA) (Leach 2001) was performed to see if the conformational changes of the protein would affect the protein accessibility to solvent and potentially to ligands. In this work the approximate probe radius of water molecule, 1.4 Å, was used to calculate the total SASA of the major states identified using PEPCAT for systems 5 and 6, as presented in Table 4.

Table 4 shows that SASA for all major states is stable within the error bars, with a slight decrease compared to the native state. This suggests that chain B became less accessible to water during the simulations under stress, with the unfolding states being slightly more compact than the starting structure. This finding is consistent with the hydrophobic nature of chain B, which would cause it to avoid contacts with water.

Hydrogen bond analysis

For each of the states identified by PEPCAT, we calculated the number of hydrogen bonds that occur within

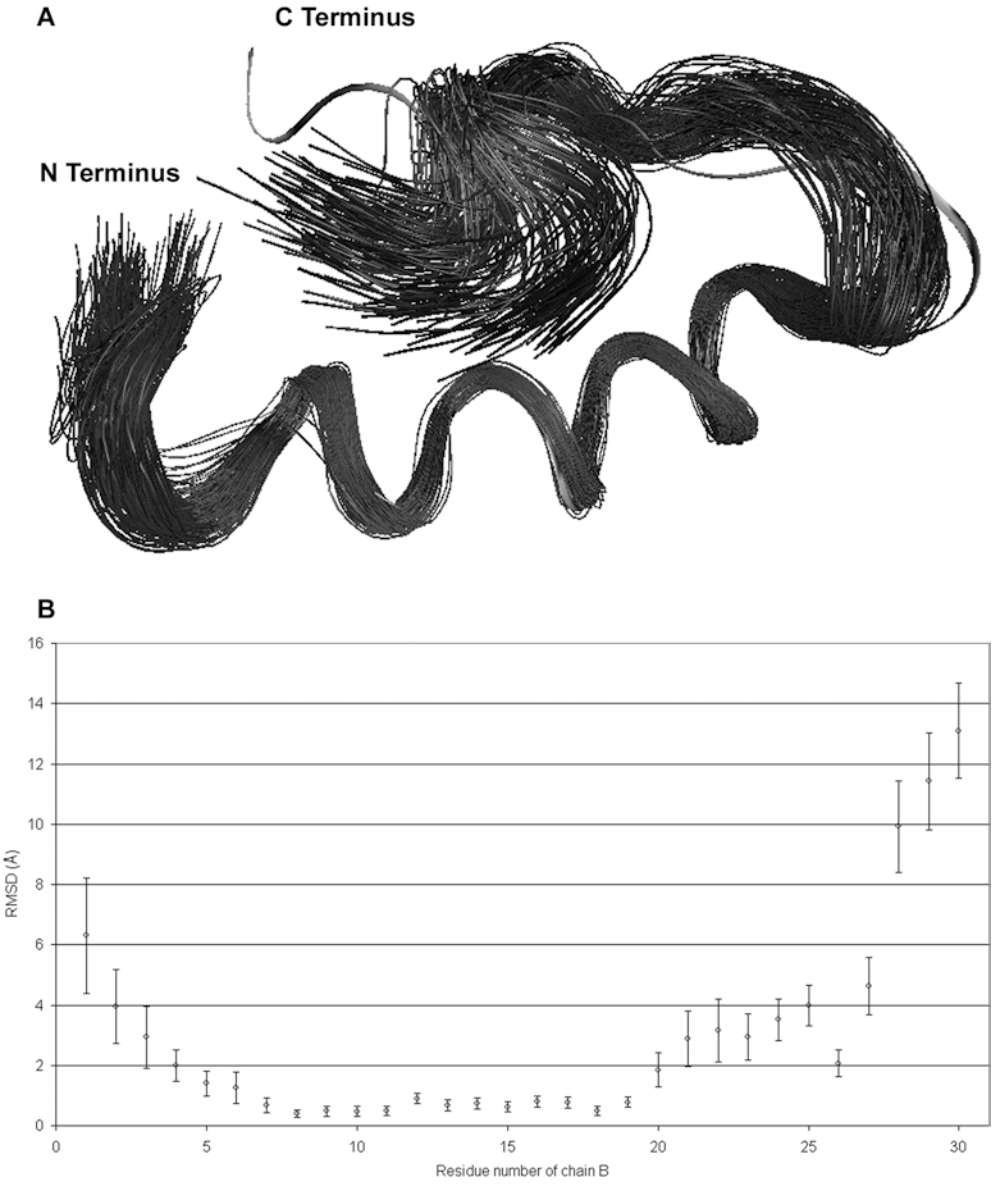

Fig. 6 **A** Snapshot of the backbone of insulin chain B, taken from the last half nanosecond (1.5–2.0 ns) of the MD simulation of the complete insulin molecule with all disulfide bonds intact at 300 K (system 1). The backbone atoms of residues 7 to 19 were aligned for this particular analysis. The *thick line* represents the backbone of the refined crystal structure, and *thin lines* represent the MD trajectory frames. **B** RMSD per residue of chain B in system 1

the protein, and between the protein and water. We have used the hydrogen bond criteria described elsewhere (Schultz and Schirmer 1979), as implemented in the InsightII software.

Table 4 shows the percentage of hydrogen bonds within the protein and between the protein and water, compared to the native state 0. This property was calculated for one representative structure from each of the major conformational states identified using PEPCAT. In general, as a protein unfolds, it presents more hydrophilic contacts to water, as reflected by the increased protein–water hydrogen bonding seen from the table. The number of internal hydrogen bonds that stabilize the secondary structure of the protein decreases with unfolding. It should be noted that state 34 shows about 15% decrease in the number of protein–water hydrogen bonds compared to the starting structure. This could be explained by the temperature effect, where the thermal motion makes the hydrogen bonds unstable.

Table 4 Properties of the major conformation states identified using PEPCAT for systems 5 and 6

State number	SASA (Å^2)	Percentage of hydrogen bonds relative to the native state	
		Protein–protein	Protein–water
0	3160 ± 80	100.0%	100.0%
3	3000 ± 80	68.4%	119.9%
4	3050 ± 100	73.7%	131.4 %
32	3080 ± 120	47.4%	153.2%
34	3070 ± 90	57.9%	86.5%

It is interesting to note the observed increase of water–protein hydrogen bonds simultaneously with the decrease of the SASA compared to the native state (Table 4). We attribute the decrease to the hydrophobic residues' coagulation, while the hydrophilic residues

become more exposed during the unfolding and thus increase the number of hydrogen bonds with water.

Conclusions

We have performed theoretical simulations and combined a number of analysis routines to investigate the conformational changes that occur in proteins as a result of thermal and chemical stresses. Using a prototype protein, insulin, we have demonstrated that such analysis can reveal important information about the protein unfolding pathways, as well as about molecular interactions that are responsible for the changes.

The simulations reproduced the equilibrium behaviour of insulin and indicated that different stress responses can be distinguished by the analysis techniques applied. In particular, it was found that the combination of thermal and chemical stresses yielded the greatest conformational response in the prototype protein.

Future work will include additional analysis methods, such as: hydrophobicity profiling of the protein, while monitoring conformational changes in order to provide additional information on the molecular mechanisms of the unfolding; simultaneous monitoring of the hydrogen bonds within the protein and between protein and water; and calculating the radius of gyration of a protein in order to monitor changes in the tertiary structure. We will apply these methods to other proteins and investigate other types of stresses. The results obtained for other proteins will be compared to experimental data for exposed proteins obtained by NMR.

Acknowledgements Useful discussions with A. Prof. John Carver (University of Wollongong, Australia), Yoke Berry (University of Wollongong, Australia), and Prof. David McKenzie (University of Sydney, Australia) are appreciated. The authors acknowledge the Australian Research Council (ARC) and Cytopia Pty. Ltd. for providing funding for this project, and the Australian Partnership for Advanced Computing (APAC) for the grant of computer time.

References

Allen MP, Tildesley DJ (1989) Computer simulation of liquids. Oxford University Press, New York

Badger J, Harris MR, Reynolds CD, Evans AC, Dodson EJ, Dodson GG, North ACT (1991) Structure of the pig insulin dimer in the cubic-crystal. Acta Crystallogr Sect B 47:127–136

Bentley G, Dodson E, Dodson G, Hodgkin D, Mercola D (1976) Structure of insulin in 4-zinc insulin. Nature 261:166–168

Berman HM, Westbrook J, Feng Z, Gilliland G, Bhat TN, Weissig H, Shindyalov IN, Bourne PE (2000) The protein data bank. Nucleic Acids Res 28:235–242

Bohr H, Bohr J (2000) Microwave-enhanced folding and denaturation of globular proteins. Phys Rev E 61:4310–4314

Brünger AT (1992) X-PLOR version 3.1, a system for X-ray crystallography and NMR. Yale University Press, New Haven

Chothia C, Lesk AM, Dodson GG, Hodgkin DC (1983) Transmission of conformational change in insulin. Nature 302:500–505

Ciszak E, Beals JM, Frank BH, Baker JC, Carter ND, Smith GD (1995) Role of C-terminal B-fragment residues in insulin assembly: the structure of hexameric LysB28ProB29-human insulin. Structure 3:615–622

Daniells C, Duce I, Thomas D, Sewell P, Tattersall J, de Pomerai DI (1998) Transgenic nematodes as biomonitors of microwave-induced stress. Mutat Res 399:55–64

de Pomerai DI, Dawe A, Djerbib L, Allan J, Brunt G, Daniells C (2002) Growth and maturation of the nematode *Caenorhabditis elegans* following exposure to weak microwave fields. Enzyme Microbial Technol 30:73–79

Derewenda U, Derewenda Z, Dodson EJ, Dodson GG, Reynolds CD, Smith GD, Sparks C, Swenson D (1989) Phenol stabilizes more helix in a new symmetrical zinc insulin hexamer. Nature 338:594–596

Derewenda U, Derewenda Z, Dodson EJ, Dodson GG, Bing X, Markussen J (1991) X-ray analysis of the single fragment B29-A1 peptide-linked insulin molecule. A completely inactive analogue. J Mol Biol 220:425–433

Dodson EJ, Dodson GG, Hubbard RE, Reynolds CD (1983) Insulin's structural behavior and its relation to activity. Biopolymers 22:281–291

Dong J, Wan Z, Popov M, Carey PR, Weiss MA (2003) Insulin assembly damps conformational fluctuations: Raman analysis of amide I linewidths in native states and fibrils. J Mol Biol 330:431–442

Du YC, Minasian E, Tregear GW, Leach SJ (1982) Circular dichroism studies of relaxin and insulin peptide fragments. Int J Pept Protein Res 20:47–55

Falconi M, Cambria MT, Cambria A, Desideri A. (2001) Structure and stability of the insulin dimer investigated by molecular dynamics simulation. J Biomol Struct Dyn 18:761–772

French PW, Donnelan M, McKenzie DR (1997) Electromagnetic radiation at 835 MHz changes the morphology and inhibits proliferation of a human astrocytoma cell line. Bioelectrochem Bioenerget 43:13–18

French PW, Penny R, Laurence JA (2000) Mobile phones, heat shock proteins and cancer. Differentiation 67:93–97

Hawkins B, Cross K, Craik D (1995) Solution structure of the B-fragment of insulin as determined by ^{1}H NMR spectroscopy. Comparison with the crystal structure of the insulin hexamer and with the solution structure of the insulin monomer. Int J Pept Protein Res 46:424–433

Hertz HG (1973) In: Franks F (ed) Water—a comprehensive treatise, vol 3. Plenum Press, New York, pp 301–399

Hua QX, Weiss MA (1991) Comparative 2D NMR studies of human insulin and des-pentapeptide insulin: sequential resonance assignment and implications for protein dynamics and receptor recognition. Biochemistry 30:5505–5515

Hua QX, Shoelson SE, Kochoyan M, Weiss MA (1991) Receptor binding redefined by a structural switch in a mutant human insulin. Nature 354:238–241

Hua QX, Shoelson SE, Inouye K, Weiss MA (1993a) Paradoxical structure and function in a mutant human insulin associated with diabetes mellitus. Proc Natl Acad Sci USA 90:582–586

Hua QX, Ladbury JE, Weiss MA (1993b) Dynamics of a monomeric insulin analogue: testing the molten-globule hypothesis. Biochemistry 32:1433–1442

Hua QX, Nakagawa SH, Jia W, Hu SQ, Chu YC, Katsoyannis PG, Weiss MA (2001) Hierarchical protein folding: asymmetric unfolding of an insulin analogue lacking the A7-B7 interfragment disulfide bridge. Biochemistry 40:12299–12311

Hua QX, Jia W, Frank BH, Phillips NF, Weiss MA (2002) A protein caught in a kinetic trap: structures and stabilities of insulin disulfide isomers. Biochemistry 41:14700–14715

Humphrey W, Dalke A, Schulten K (1996) VMD – visual molecular dynamics. J Mol Graph 14:33–38

InsightII User Guide (1996) Molecular Simulations, San Diego, Calif

Kalé L, Skeel R, Bhandarkar M, Brunner R, Gursoy A, Krawetz N, Phillips J, Shinozaki A, Varadarajan K, Schulten K (1999) NAMD2: Greater scalability for parallel molecular dynamics. J Comput Phys 151:283–312

Kazmirski SL, Daggett V (1998) Simulations of the structural and dynamical properties of denatured proteins: the "molten coil" state of bovine pancreatic trypsin inhibitor. J Mol Biol 277: 487–506

Kazmirski SL, Li A, Daggett V (1999) Analysis methods for comparison of multiple molecular dynamics trajectories: applications to protein unfolding pathways and denatured ensembles. J Mol Biol 290:283–304

Kruger P, Strassburger W, Wollmer A, van Gunsteren WF, Dodson GG (1987) The simulated dynamics of the insulin monomer and their relationship to the molecule's structure. Eur Biophys J 14:449–459

Laurence JA, French PW, Lindner RA, McKenzie DR (2000) Biological effects of electromagnetic fields – mechanism for the effects of pulsed microwave radiation on protein conformation. J Theor Biol 206:291–298

Leach AR (2001) Molecular modelling – principles and applications, 2nd edn. Prentice-Hall, Harlow, UK

Li A, Daggett V (1996) Identification and characterization of the unfolding transition state of chymotrypsin inhibitor 2 by molecular dynamics simulations. J Mol Biol 257:412–429

Li A, Daggett V (1998) Molecular dynamics simulation of the unfolding of barnase: characterization of the major intermediate. J Mol Biol 275:677–694

Ludvigsen S, Olsen HB, Kaarsholm NC (1998) A structural switch in a mutant insulin exposes key residues for receptor binding. J Mol Biol 279:1–7

MacKerell AD Jr, Bashford D, Bellott M, Dunbrack RL Jr, Evanseck JD, Field MJ, Fischer S, Gao J, Guo H, Ha S, Joseph-McCarthy D, Kuchnir L, Kuczera K, Lau FTK, Mattos C, Michnick S, Ngo T, Nguyen DT, Prodhom B, Reiher WE III, Roux B, Schlenkrich M, Smith JC, Stote R, Straub J, Watanabe M, Wiórkiewicz-Kuczera J, Yin D, Karplus M (1998) All-atom empirical potential for molecular modeling and dynamics studies of proteins. J Phys Chem B 102:3586–3616

Mark AE, Berendsen HJ, van Gunsteren WF (1991) Conformational flexibility of aqueous monomeric and dimeric insulin: a molecular dynamics study. Biochemistry 30:10866–10872

Mayor U, Johnson CM, Daggett V, Fersht AR (2000) Protein folding and unfolding in microseconds to nanoseconds by experiment and simulation. Proc Natl Acad Sci USA 97:13518–13522

Mirmira RG, Nakagawa SH, Tager HS (1991) Importance of the character and configuration of residues B24, B25, and B26 in insulin-receptor interactions. J Biol Chem 266:1428–1436

O'Donohue MF, Burgess AW, Walkinshaw MD, Treutlein HR (1995) Modeling conformational changes in cyclosporin A. Protein Sci 4:2191–2202

O'Donohue M, Minasian E, Leach SJ, Burgess AW, Treutlein HR (2000) PEPCAT – a new tool for conformational analysis of peptides. J Comput Chem 21:446–461

Olsen HB, Ludvigsen S, Kaarsholm NC (1996) Solution structure of an engineered insulin monomer at neutral pH. Biochemistry 35:8836–8845

Pande VS, Rohksar DS (1999) Molecular dynamics simulations of unfolding and refolding of a β-hairpin fragment of protein G. Proc Natl Acad Sci USA 96:9062–9067

Pastrana-Rios B (2001) Mechanism of unfolding of model helical peptide. Biochemistry 40:9074–9081

Pittman IT, Tager HS (1995) A spectroscopic investigation of the conformational dynamics of insulin in solution. Biochemistry 34:10578–10590

Qiao ZS, Min CY, Hua QX, Weiss MA, Feng YM (2003) In vitro refolding of human proinsulin. Kinetic intermediates, putative disulfide-forming pathway folding initiation site, and potential role of C-peptide in folding process. J Biol Chem 278:17800–17809

Schultz GE, Schirmer RH (1979) Principles of protein structure. Springer, New York

Snow CD, Nguyen H, Pande VS, Gruebele M (2002) Absolute comparison of simulated and experimental protein-folding dynamics. Nature 420:102–106

Stuerga DAC, Galliard P (1996) Microwave athermal effects in chemistry: a myth's autopsy. J Microwave Power Electromagn Energy 31:87–100

Wu C-S, Yang JT (1981) Conformation of insulin and its fragments in surfactant solutions. Biochim Biophys Acta 667:285–293

Yao ZP, Zeng ZH, Li HM, Zhang Y, Feng YM, Wang DC (1999) Structure of an insulin dimer in an orthorhombic crystal: the structure analysis of a human insulin mutant (B9 Ser $\rightarrow$ Glu). Acta Crystallogr Sect D 55:1524–1532

Zhang Y, Whittingham JL, Turkenburg JP, Dodson EJ, Brange J, Dodson GG (2002) Crystallization and preliminary crystallographic investigation of a low-pH native insulin monomer with flexible behaviour. Acta Crystallogr Sect D 58:186–187